ACS OMEGA

Article

Cite This: ACS Omega 2018, 3, 9146−9154

http://pubs.acs.org/journal/acsodf

Large-Scale Fabrication of High-Performance Ionic Polymer−Metal Composite Flexible Sensors by in Situ Plasma Etching and Magnetron Sputtering

Ruoping Fu,[†,‡] Ying Yang,[‡] Chao Lu,[‡] Yue Ming,[‡] Xinxin Zhao,[‡] Yimin Hu,[‡] Lei Zhao,[‡] Jian Hao,[†] and Wei Chen*[,‡,§]

[†]Department of Chemistry, College of Sciences, Shanghai University, Shanghai 200444, P. R. China

[‡]i-Lab, Suzhou Institute of Nano-Tech and Nano-Bionics, Chinese Academy of Sciences, Suzhou 215123, P. R. China

[§]Nanotechnology Centre for Intelligent Textiles and Apparel, Institute of Textiles and Clothing, The Hong Kong Polytechnic University, Kowloon, Hong Kong 999077, P. R. China

Supporting Information

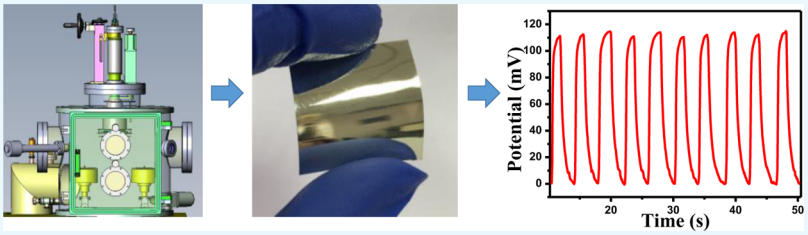

ABSTRACT: Flexible electronics has received widespread concern and research. As a most-fundamental step and component, polymer metallization to introduce conductive electrode is crucial in successful establishment and application of flexible and stretchable electronic system. Ionic polymer−metal composite (IPMC) is such an attractive flexible mechanical sensor with significant advantages of passive and space-discriminative capability. Generally, the IPMC sensor is fabricated by the electroless plating method to form structure of ionic polymer membrane sandwiched with two metallic electrodes. In order to obtain high-quality interface adhesion and conductivity between polymer and metal, the plating process for IPMC sensor is usually time-consuming and uncontrollable and has low reproducibility, which make it difficult to use in practice and in large-scale. Here, a manufacturable method and equipment with short processing time and high reproducibility for fabricating IPMC sensors by in situ plasma etching and magnetron sputtering depositing on flexible substrates is developed. First, the new method shortens the fabrication period greatly from 2 weeks to 2 h to obtain IPMC sensors with sizes up to 9 cm × 9 cm or arrays in various patterns. Second, the integrated operation ensures all sample batch stability and performance repeatability. In a typical IPMC sensor, nearly 200 mV potential signal due to ion redistribution induced by bending strain under 1.6% can be produced without any external power supply, which is much higher than the traditional electroless plating sensor. This work verified that the in situ plasma etching and magnetron sputtering deposition could significantly increase the interface and surface conductivity of the flexible devices, resulting in the present high sensitivity as well as linear correlation with strain of the IPMC sensor. Therefore, this introduced method is scalable and believed to be used to metalize flexible substrates with different metals, providing a new route to large-scale fabrication of flexible devices for potential wearable applications in real-time monitoring human motion and human−machine interaction.

INTRODUCTION

In order to overcome application problems of the electronic system in the large deformation and arbitrarily curved surfaces, flexible electronics that is compatible with movable parts has been driven to the advent and growth over the last few decades. Flexible electronics create a wide range of revolutionary functional devices, including sensors, actuators, robots, and other electronic devices that are bendable, curved, and even stretchable.[1−9] As the most basic component of electronics, the thin-film conductive electrode of polymer metallization fabrication has become a key part of the successful application of flexible and stretchable electronic systems. Recently, ionic polymer−metal composites (IPMCs) have extensively been studied for their excellent properties and potential applications in the areas of science and technology as flexible sensors.[10−16] An IPMC sample typically consists of a thin ion-exchange membrane (e.g., Nafion) and metallic electrodes on both surfaces with a noble metal.[17] Also, IPMC can induce voltages by bending or stretching the membrane, which makes IPMC an ideal flexible sensor.

Received: May 2, 2018
Accepted: August 1, 2018
Published: August 15, 2018

DOI: 10.1021/acsomega.8b00877
ACS Omega 2018, 3, 9146−9154

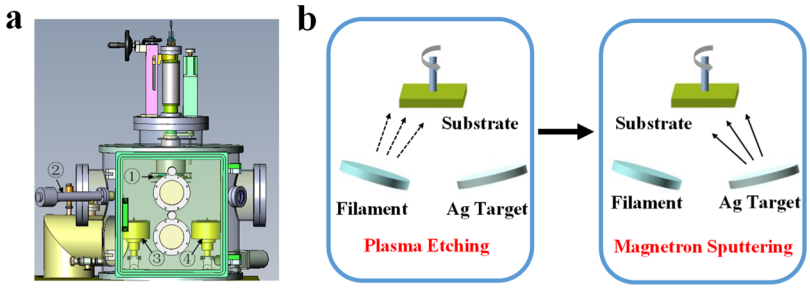

Figure 1. Schematic of the fabrication process. (a) Equipment used to manufacture the IPMC sensor. (b) Schematic of the fabrication process of the IPMC sensor.

Compared with electronic sensors,[18−20] these IPMC sensors show significant advantages of no power supply and the ability to distinguish bending directions.

IPMC sensors are generally fabricated by electroless plating[21] to achieve polymer metallization on the flexible Nafion membrane. Polymer metallization use conventional conductive materials, such as rigid metal nanoparticles (mainly including Cu, Ag, or Au) on polymer film to realize flexibility and stretchability. However, these conductive materials may not be suitable for flexible electronics. The flexible polymeric material (from fractions to hundreds of MPa) and the hard electrode material (from tenths to hundreds of GPa)[22] have the large Young's modulus mismatch, which causes electrode cracking, stripping, and delamination during multicycle bending and further limits the lifetime and the bending stability of the IPMC sensors.[23] Thus, in view of applications, fabrication of compliant and well-adherent electrodes that are closely integrated with the polymer layer is crucial.[24] Besides, fabrication of IPMC sensors still remains a big challenge mainly because the traditional electroless plating method is manual operation. This process not only consumes a long period, but it also has many uncontrollable factors. Most importantly, reliability of manual operation is not strong, resulting in low reproducibility. What's more, they have difficulty for batch production. Therefore, in order to develop production techniques of industrial interest, a non-manual preparation method with high efficiency should be developed.

Here, in order to solve the aforementioned problems, we develop a manufacturable and integrative method and equipment with short processing time and high reproducibility for fabricating IPMC sensors by in situ plasma etching and magnetron sputtering depositing on flexible substrates. Some literature studies have only used plasma to etch Nafion membrane. Omosebi and Besser[25] used plasma to etch the Nafion membrane for multiple electrochemical applications. Van Nguyen[26] etched with argon on the surface Nafion membrane and investigated its performance in a proton-exchange membrane fuel cell. Also, some literature studies have only reported to prepare IPMC using magnetron sputtering. Zhou[27] sputter-coated a gold seed layer of 0.4 μm thickness. Siripong[28] employed sputter coating for deposition of gold on Nafion for fast and economical fabrication of IPMC. Thus, we place two devices into a single chamber to rapidly and large-scale prepare IPMC. Plasma etching is a potentially attractive method to control polymer surface modification without affecting the bulk properties of the material.[29] Plasma treatment depends heavily on the adjustment of parameters such as power and treatment duration.[30] We can quantify and repeat the degree of etching with defined parameters. Magnetron sputtering has developed rapidly over the last decades to the point where it has become established as the process of choice for the deposition of a wide range of industrially important coatings on plastic substrates at room temperature.[31] For equipment, plasma etching filament and magnetron sputtering target are installed in one chamber and the control panel was operated to achieve the integrative fabrication. Plasma etching increases the roughness of the intermediate layer surface to improve the adhesion of the electrode layer. Magnetron sputtering deposits silver particles to metallize Nafion membrane. Silver is considered as a high conductive material and is much cheaper than gold, platinum, or other precious metals.

The integrative preparation method provides the possibility of batch and reproducible production of flexible IPMC sensors. First, the new method shortens the fabrication period greatly from 2 weeks to 2 h to obtain IPMC sensors with sizes up to 9 cm × 9 cm or arrays in various patterns. Second, the integrated operation ensures all sample batch stability and performance repeatability. In a typical IPMC sensor, nearly 200 mV potential signal under a bending-induced strain as small as 1.6% can be produced without any external power supply, which is 63 times higher than that of the sensor fabricated by traditional electroless plating. We verified that the in situ plasma etching and magnetron sputtering depositing could significantly increase the interface and surface conductivity of the flexible devices. Plasma etching processing improves the degree and uniformity of etching on the Nafion film surface, resulting in a much lower equivalent series resistance. The magnetron sputtering-based sensor shows a good interface contact between the electrolyte and electrode as well as excellent electronic conductivity of the electrode material. Moreover, this flexible IPMC sensor has better bending cycle stability and high sensitivity as well as linear correlation with strain. Then, we mainly optimize the parameters of etching power, etching time and magnetron sputtering, sputtering time, sputtering power, working pressure, and working argon flow rate to get an IPMC sensor with excellent performance. In a word, this introduced method is scalable and believed to be used to metalize flexible substrates with different metals, providing a new route to large-scale fabrication of flexible devices for potential wearable applications in real-time monitoring human motion and human−machine interaction.

RESULTS AND DISCUSSION

Preparation and Characterization. The equipment used to fabricate the flexible IPMC sensor is shown in Figure 1a. The sample holder (①), the filament (③) for plasma etching, and the magnetron sputtering target (④) are installed in the chamber of the equipment. The equipment is also equipped

DOI: 10.1021/acsomega.8b00877
ACS Omega 2018, 3, 9146−9154

with a mechanical handle (②) for inverting the sample on the sample holder, which ensures that both sides of the sample are plasma-etched and magnetron sputtering-coated with silver particles to achieve integrative fabrication. In the fabrication process, we only need to operate and set the plasma etching and magnetron sputtering parameters on the control panel instead of manual operation, which is a simple and controllable process. A schematic representation of the fabrication process of the flexible IPMC sensor is presented in Figure 1b. Before plasma etching, the Nafion substrate (suitable for different sizes and array pattern) is fixed on the hollow part of rotatable sample holder allowing the rotation of the substrate along a direction, which assures sample uniformity of etching and metalizing over the entire surface. The picture of simple holder is shown in Figure S1. Then, plasma etching with defined energy is used to control Nafion membrane surface modification. After completing, the holder is turned over 180° by the mechanical handle, and the opposite side of the Nafion polymer is processed. Finally, magnetron sputtering deposited silver particles on the metallic Nafion polymer. Once the electrode with appropriate conductivity has been deposited, the holder is turned over 180° by the mechanical handle, and the opposite side of the Nafion polymer is deposited with silver particles. The details can be found in the Experimental Methods section.

The pictures of fabricated IPMC sensors are shown in Figure 2. The IPMC sensor is flexible and can be easily bent.

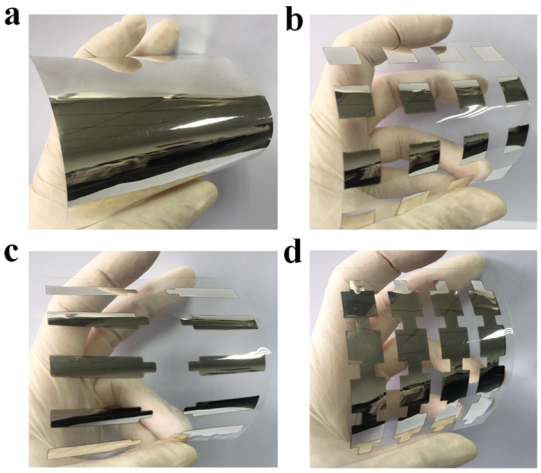

Figure 2. Pictures of the fabricated IPMC sensors. (a) Pictures of large-scale IPMC sensors. (b–d) Pictures of various array patterns of IPMC sensors.

What's more, the specular IPMC sensor surface is shiny and bright; in other words, the fabricated silver electrode layer has very high quality. We can obtain IPMC sensors with size up to 9 cm × 9 cm (Figure 2a) or arrays in various patterns (Figure 2b–d). Moreover, mechanical operation ensures high performance of each batch samples.

Then, the observation of microscopic morphology of the IPMC sensor is done by using an electron microscope. Figure 3a displays the scanning electron microscopy (SEM) image of the IPMC sensor surface, which clearly shows the homogeneous silver layer coated on the surface of the polymer membrane layer and the silver nanoparticles are closely integrative, having a diameter between 50 and 160 nm. Figure 3b displays a detail of the cross-sectional SEM image of the IPMC sensor, which clearly indicates that the silver nanoparticle layer and the Nafion membrane interlayer are well-interconnected. The structure benefits the cyclic stability of the sensor. In the inset of Figure 3c, the Nafion membrane interlayer with an average thickness of 183 μm is sandwiched between two silver electrodes, forming the IPMC sensor. In order to verify the distribution of the Ag electrode layer in the IPMC sensor, Figure 3c shows the energy-dispersive X-ray spectroscopy (EDX) signal, which is collected from the vertical cross section of the IPMC in the inset SEM image. Ag is mainly concentrated on both sides of IPMC. Moreover, typical X-ray diffraction (XRD) powder diffraction pattern of the surface layer of the IPMC sensor is shown in Figure 3d. The peaks at 38.1°, 44.21°, 64.44°, and 77.33° correspond to the (111), (200), (220), and (311) crystalline planes of the face-centered cubic crystal structure of Ag (JCPDS, file no. 04-0783), which demonstrates the existence of Ag electrode layer.

Sensing Performance of the IPMC Sensor. An IPMC sample typically consists of a thin ion-exchange membrane and a noble metal as electrodes on both surfaces. Figure 4a displays the sensing mechanism of the IPMC sensor. As we know, the Nafion membrane contains the sulfonic acid group and can be ionized and release the mobile hydrions with adsorbed water. When the sensor is in a flat state, mobile hydrions uniformly disperse in the Nafion membrane. When a bend deformation is applied on the sensor, an elastic stress gradient is generated along the thickness. The mobile hydrions on the compressed side of the membrane migrate and accumulate on the lower hydraulic pressure side of the membrane. More hydrions accumulate on the stretched side, resulting in a positive potential. The voltage signal is generated from ion movement and accumulation in the deformation process, so the sensor could generate electrical signal without external energy supply.

For the sensing mechanism of the sensor, we buit a corresponding test platform and obtained signals of sensors under different strains. The test method can be found in the Experimental Methods section. The output electrical signals of magnetron sputtering depositing silver particle-based sensor and conventional electroless plating-based sensor are shown in Figure 4b. Output voltage shows a periodic alternation of positive voltage, and output voltage of the magnetron sputtering sensor is 112.55 mV. However, when the IPMC sensor returns back after bending, hysteresis is produced because the movement of the ions is not as fast as electron transport. Thus, the signal peak is asymmetric. Output potential of the electroless plating sensor is 1.80 mV. The signal of magnetron sputtering is much larger than that of the electroless plating sensor. The ability of the IPMC sensor to recognize the orientation is shown in Figure 4c. The insets in Figure 4c display the real operation scenes of upward-bending and downward-bending in the test process. For the first six times, the sensor bends downward to get the negative voltage, and for the latter six times, the sensor bends up and gets a positive voltage. As the sensor bends to opposite directions, positive and negative relative potentials appear in turn, respectively. A series of bending deformations of 1, 2, 3, 4, 5, 6, and 7 mm are repeatedly measured (Figure 4d). Different displacements produce different signals, indicating high repeatability and sensibility of IPMC sensors.

We use the Euler–Bernoulli theory to build a model to calculate the strain at the corresponding displacement. The film sensor has a thickness of h and a length of L. When the displacement platform moves x, the film is curved. A schematic

DOI: 10.1021/acsomega.8b00877
ACS Omega 2018, 3, 9146–9154

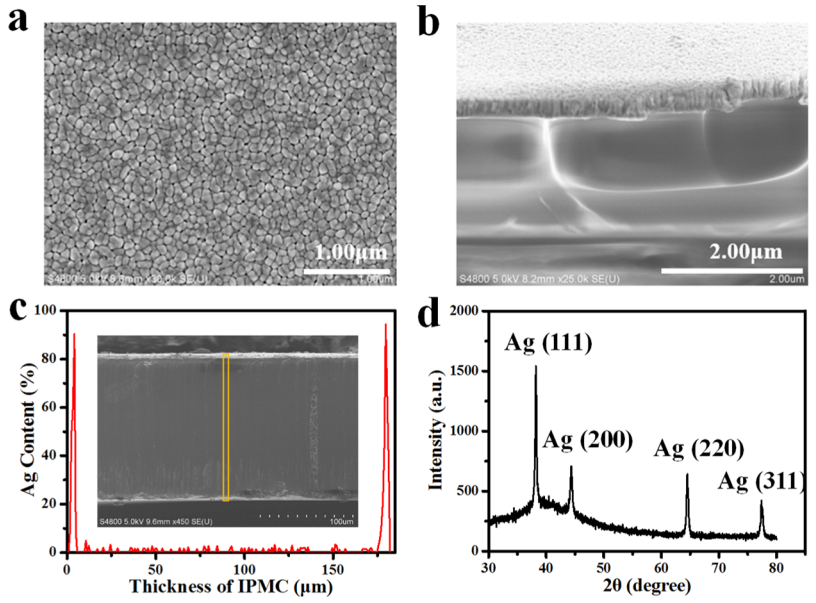

Figure 3. Characterization of the morphology of the IPMC sensor. (a) SEM image of the IPMC sensor surface. (b) Cross-sectional SEM image of the IPMC sensor. (c) EDX line scan of the cross section of the IPMC sensor. The inset shows the corresponding SEM image. (d) Typical XRD pattern of the surface layer of the IPMC sensor.

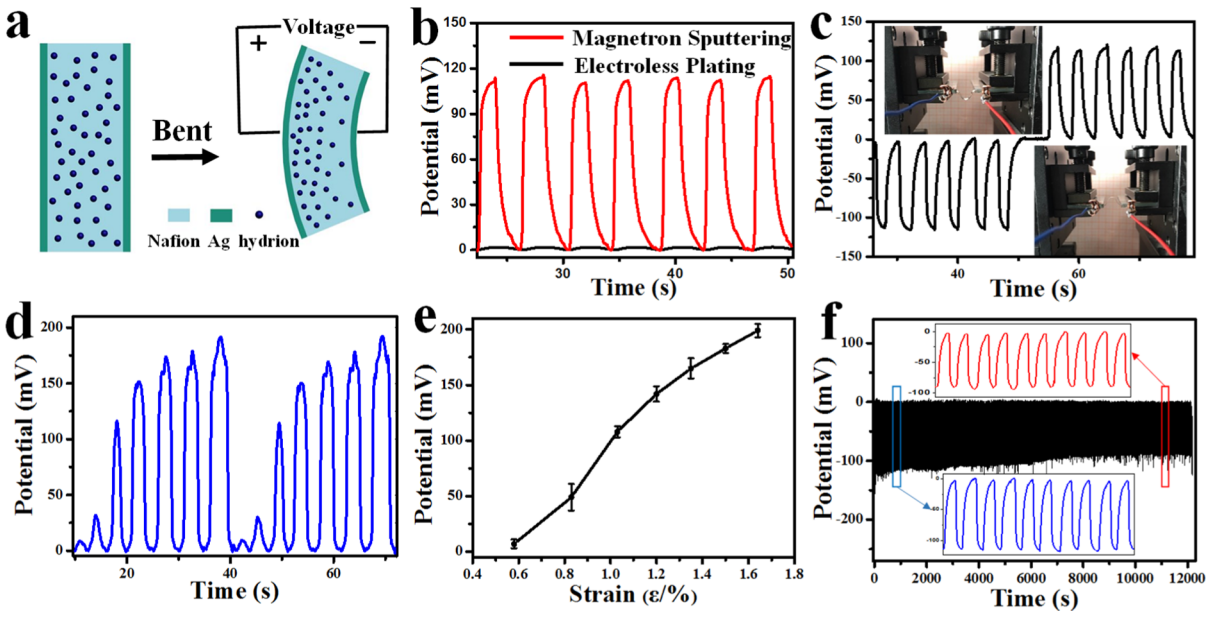

Figure 4. Sensing mechanism and sensing performance of IPMC sensors. (a) Schematic of the sensing mechanism. (b) Potential of the in situ plasma etching and magnetron sputtering depositing silver particle-based IPMC sensor and the electroless plating-based IPMC sensor. (c) Voltage responses of the IPMC sensor to the recognization of the bending direction. (d) Potential of the sensor with variations of the bending deformation of 1, 2, 3, 4, 5, 6, and 7 mm. (e) Potential signal of the sensor vs strain (ε). (f) Bending and recovery of the IPMC sensor for 3000 cycles of 3 mm displacement.

diagram is shown in Figure S2. Assuming that the central angle of the curved arc is θ, the radius is R. According to the geometric relations, we can list the equations

$$\theta \times R = L \tag{1}$$

$$2R \times \sin\frac{\theta}{2} = L - x \tag{2}$$

We know L and x and can get θ and R from eqs 1 and 2. Finally, the Euler−Bernoulli approximation theory is used to calculate the bending strain, and the strain corresponding to the displacement is obtained.

$$\varepsilon = \frac{h}{2R} \tag{3}$$

Using this method, the strain of our IPMC is 1.03% at a displacement of 3 mm.

Potential signal as a function of a series of strain is given in Figure 4e, which exhibits an approximately linear correlation. Small error bars (standard deviations) are taken from 10 times measurement. Therefore, the IPMC sensor has perfect

DOI: 10.1021/acsomega.8b00877
ACS Omega 2018, 3, 9146−9154

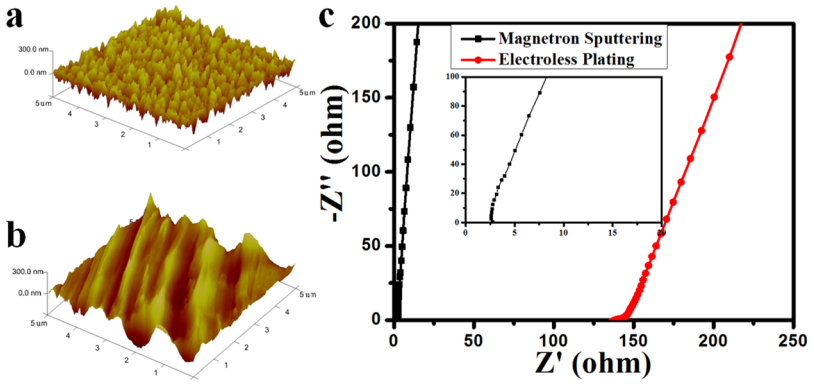

Figure 5. (a) 3D AFM image of the plasma etching-based Nafion membrane. (b) 3D AFM image of the manual processing-based Nafion membrane. (c) Nyquist plots of three electrodes of the IPMC sensor with electroless plating and the IPMC sensor with magnetron sputtering. The inset picture clearly displays Nyquist plots of three electrodes of the IPMC sensor with magnetron sputtering.

repeatability. The sensor potential under the maintained extended state is also detected (Figure S3). When the sensor keeps bending, the signal continues to increase and then begins to fall slowly. The output signal declines around 5% slowly when the sensor maintained 10 s bending state (Figure S3a). The output signal declines around 27.5% while maintaining 60 s bending state (Figure S3b). In order to analyze the durable performance of the IPMC sensor, cyclical bending deformation and recovery of the sensor was measured for 3000 cycles of 3 mm displacement and is shown in Figure 4f. The insets in Figure 4f show the details of the cyclic test. The output potential signals of the sensor are stably maintained with a relative small variation. Although the signal has slight attenuation, the signal is still much larger than the signal of the electroless plating-based sensor, and the peak type is consistent. It is proved that the sensors have a relatively good cycle stability. Therefore, the sensor fulfills the requirement for practical application. This is the result of our preliminary experimental stage. In the future, we will continue to explore and improve its durable performance. The electromechanical behavior of IPMC under electrical voltage stimulation of ±1 V is also investigated (Figure S4). The bending displacement is monitored by a laser displacement meter. Bending displacement reaches 11.0 μm. The size of the mobile ions in the IPMC is small. If we increase the number of mobile ions and soak large-size ions in the Nafion membrane, the electromechanical behavior of IPMC will be improved.

The traditional method for preparing an IPMC sensor is manual processing for roughing Nafion film and electroless plating for electrode layers. The signal of our sensor (112.55 mV, Figure 4b) is about 63 times compared with that of electroless plating-based sensor (1.80 mV, Figure 4b). We read the relevant literature studies and found that the signal of the sensor made by electroless plating is relatively low. The IPMC sensor prepared by Song[32] can generate a voltage signal of 20 mV. This is the largest signal of IPMC we have seen from the literature so far. However, the signal of our IPMC sensor is much larger than this value. The electrode layer thickness of the electroless plating-based IPMC sensor is about 3−5 μm. The electrode layer thickness of the magnetron sputtering-based IPMC sensor is 280−300 nm. For the electroless plating-based IPMC sensor, the impregnation−reduction steps were repeated five times. The reduction step is a process of electrode layer growth, and the reduction takes a total of 25 h. The growth rate is 0.12−0.2 μm/h. For the magnetron sputtering-based IPMC sensor, magnetron sputtering lasts for 30 min and the electrode layer thickness increases to 280−300 nm. The growth rate is 0.56−0.6 μm/h. In order to evaluate the effect of the in situ etching and magnetron sputtering depositing method to increase potential signal, first, the average root mean square (rms) surface roughness (R_q) value of the treated Nafion membrane is measured and analyzed. Figure 5a,b shows 3D atomic force microscopy (AFM) images of Nafion membrane of plasma etching processing and manual processing, respectively. The average R_q value of Nafion membrane of plasma etching processing is about 72.9 nm. The measured R_q value for manual processing Nafion membrane is about 65.6 nm and is relatively lower. It is clear from the AFM image that surface grooves of the plasma etching-treated membrane are evenly distributed and have comparatively consistent depth compared with those of the manual processing membrane, which greatly benefits for the proper microstructural development. The observed more uniform rough surface is a desirable two-dimensional layer by layer growth mode (Frank−van der Merwe mode).[33] Figure 5c shows Nyquist plots of the IPMC sensors. The equivalent series resistance of the magnetron sputtering-based IPMC sensor is 2 Ω, which is much lower than that of electroless plating-based sensor (equivalent series resistance of is 145 Ω). The magnetron sputtering-based IPMC sensor shows a good interface contact between the electrolyte and electrode as well as excellent electronic conductivity of the electrode material. The surface sheet resistance of the electrode film is as high as 0.08−0.15 Ω/□, further confirming excellent electronic conductivity. In summary, it is proved that the in situ plasma etching and magnetron sputtering depositing method is effective for fabricating high-performance IPMC sensors.

However, the plasma etching power and duration have a great influence on the degree and uniformity of the film surface etching. In addition, magnetron sputtering time, sputtering power, working pressure, and working argon flow rate also have great impact on the performance of the sensor. Consequently, the conditions of the preparation process are optimized to obtain excellent IPMC sensors. Cho et al.[34] studied that the etching procedure did not alter the chemical character of the membrane. Only the physical roughness does not affect performance. The surface morphologies of the modified Nafion membranes are investigated by using SEM, as shown in Figure 6a−i. The surface roughness enhances with increase of power (Figure 6a−f) or time (Figure 6g−i) because

DOI: 10.1021/acsomega.8b00877
ACS Omega 2018, 3, 9146−9154

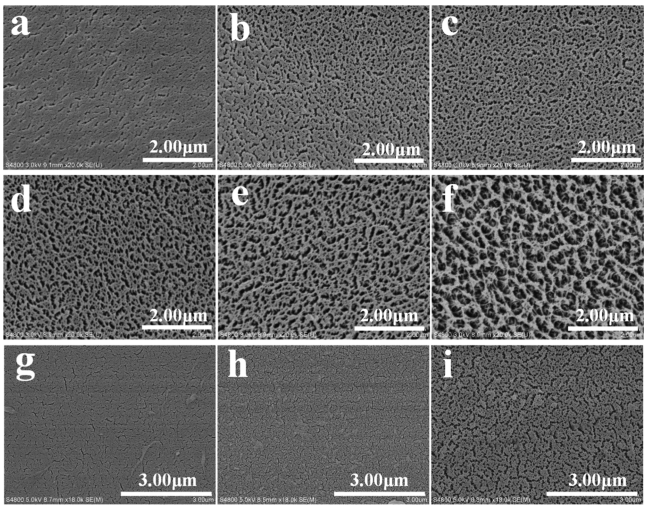

Figure 6. SEM images of different plasma etching powers and constant 180 s etching duration on the Nafion membrane surface: (a) 8 W; (b) 10 W; (c) 12 W; (d) 14 W; (e) 16 W; and (f) 18 W. SEM images of different plasma etching durations and constant 14 W etching power on the Nafion membrane surface: (g) 180 s; (h) 360 s; and (i) 540 s.

of the effect of the plasma etching treatment. Output potential signals of IPMC sensors of different plasma etching powers or time can be used as a parameter to determine the best conditions, which is shown in Figure 7a,b. When the etching power is 8 or 10 W, the prepared sensor cannot obtain a stable output signal. The output signal increases to the maximum and then significantly goes down as the etching power increases. When the etching time is 360 s, the sensor has maximum output signal. The Nafion membrane surface can be etched efficiently, which affects the output signal of IMPC.

In the same method, the effects of sputtering time, sputtering power, working pressure, and working argon flow rate on the film performance are tested with indicators such as electrode layer thickness and output potential signal while keeping other parameters constant.

Figure 8a shows output potential signals and electrode layer thicknesses of sensors under different sputtering power. In a certain range, the greater the sputtering power, the deposited particles have higher energy and the metal element deposition on the substrates is accelerated. Therefore, the particles have higher adhesion with the substrate. The film thickness increases with the increase of sputtering power. Output potential signal reaches the maximum value at 100 W power; the value of the output potential is an important parameter of device performance. Therefore, the sputtering power at 100 W is considered as a better value to ensure outstanding sensor performance.

Figure 8b depicts output potential signals and electrode layer thicknesses of sensors under different sputtering times. It is observed that the electrode layer thickness increases with increase of sputtering time. To be more specific, with the increase of sputtering time, the content of silver increases. The number of particles deposits onto the Nafion substrate increases. ZAO films were prepared by magnetron sputtering conducted by Song,[35] who has already shown that for a longer sputtering time, the thickness of the film increases as well, and interestingly shows a linear correspondence to sputtering time. Output potential signal reaches the maximum value at 30 min. With a shorter deposition time, there are less particles on the substrate. As the deposition time increases, the number of particles increases, and the layer thickens. The electrode layer has good compactness. However, with a longer deposition time, the electrode layer thickness increases, which is not conducive to sensors bending deformation. The electrode is easy to peel and split as the thickness increases. Thus, the sputtering time at 30 min is considered as a better value to ensure sensor performance excellent.

It can be seen from Figure 8c that with the increase of working pressure, the electrode layer thickness decreases. With a lower deposition pressure, there are less collisions in the path of particles to the substrate. Particles can easily reach the substrate to form a film and the film has good performance. However, when the deposition pressure increases, there are more collisions in the path of particles to the substrate, thus the particles energy decreases. The amount of particles reaching the substrate decreases, which causes more defects in the films and leads to the decrease of electrode layer thickness. Output potential signal of sensor increases from 2.2 mV (0.25 Pa) to a maximum value at 29.4 mV (1.0 Pa) and then goes down to 9.5 mV at 3.4 Pa. Considering appropriate electrode layer thickness and electrical signals, the sensor performance is more excellent when the deposition pressure at 1.3 Pa.

Figure 8d shows the variety of electrode layer thicknesses and output potential signals of sensors as a function of different the argon flow rate. Apparently, the electrode layer thickness decreases with the increase of argon flow rate. When the magnetron sputtering starts, the electrons collide with the argon atoms in the process of flying to the substrate under the action of the electric field and produce argon ions and new

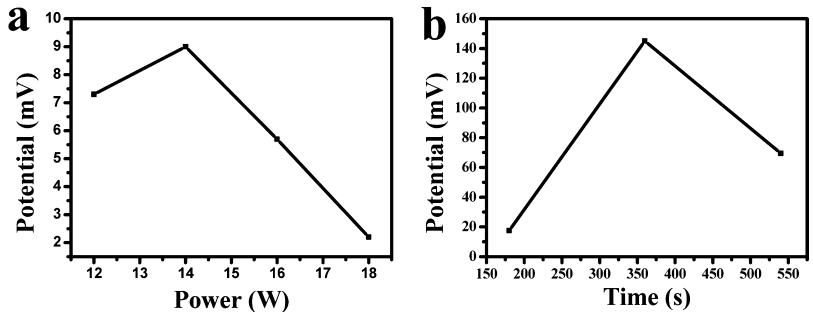

Figure 7. (a) Output potential signals of IPMC sensors of different plasma etching powers and constant 180 s etching duration on the Nafion membrane surface. (b) Output potential signals of IPMC sensors of different plasma etching durations and constant 14 W etching power on the Nafion membrane surface.

DOI: 10.1021/acsomega.8b00877
ACS Omega 2018, 3, 9146−9154

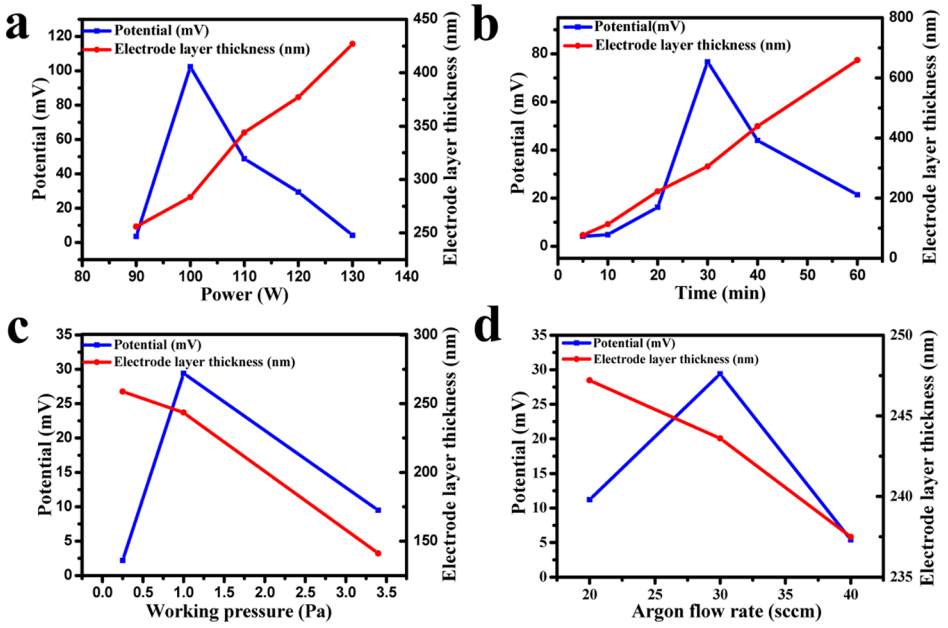

Figure 8. Curve of output potential signals and electrode layer thicknesses of sensors under different magnetron sputtering conditions: (a) 90−130 W different sputtering power and constant sputtering 30 min duration, 1.0 Pa working pressure, 30 sccm argon flow rate; (b) 5−60 min different sputtering time and constant sputtering 120 W power, 1.0 Pa working pressure, 30 sccm argon flow rate; (c) 0.25−3.5 Pa different sputtering working pressure and constant sputtering 120 W power, 30 min duration, 30 sccm argon flow rate; and (d) 20−40 sccm different sputtering argon flow rate and constant sputtering 120 W power, 30 min duration, 30 sccm argon flow rate.

electrons. Argon ions in the electric field accelerate toward the cathode target and high-energy bombard the target surface, and the target sputtering occurred. Neutral target atoms or molecules are deposited on the substrate to form a thin film. The higher argon flow rate increases the working pressure, and there is lower mobility and a great number of native defects. The output potential signal of the sensor rises to a peak value at an argon flow rate of 30 sccm and then decreases as the argon flow rate further increases.

From inspection, the maximum voltage signal is found to be 29.55 mV for the sample grown using an argon flow rate of 30 sccm. Considering the stability of the sensors and the output of the electrical signal, the optimal argon flow rate is 28 sccm.

CONCLUSIONS

In this work, an Ag electrode-based IPMC sensor is fabricated on a flexible Nafion substrate by the in situ plasma etching and dc balanced magnetron sputtering deposition technique. The new method shortens the fabrication period greatly from 2 weeks to 2 h to obtain IPMC sensors with sizes up to 9 cm × 9 cm or arrays in various patterns. The integrated operation ensures all sample batch stability and performance repeatability. These IPMC sensors can generate electrical signals under the external bending deformation for mobile hydrions migrate and accumulate on the lower hydraulic pressure side. IPMC sensors we fabricated can generate nearly 200 mV potential signal without external power supply under a 1.6% bending-induced strain and recognize different directions of the bending strain. The signal of our sensor is much larger than that of the traditional electroless plating-based sensor. What's more, this IPMC sensor is suitable for in long-term and large-scale bending and have high sensitivity as well as linear correlation with strain.

The plasma etching-based Nafion membrane has higher rms surface roughness (R_q) values. Surface grooves of membrane are evenly distributed and have comparatively consistent depth. The equivalent series resistance of the magnetron sputtering-based IPMC sensor is 2 Ω, which is much lower than that of the electroless plating-based sensor (equivalent series resistance of is 145 Ω). The magnetron sputtering-based sensor shows a good interface contact between the electrolyte and electrode as well as excellent electronic conductivity of the electrode material. Optimal properties of the IPMC sensor are obtained with plasma etching power at 14 W, plasma etching duration at 360 s, magnetron sputtering power at 100 W, magnetron sputtering time at 30 min, magnetron sputtering working pressure at 1.3 Pa, and a magnetron sputtering working argon flow rate at 28 sccm. From these data, the IPMC sensor fabricated by in situ plasma etching and magnetron sputtering has high performance of large and stable output signal. The study provides a manufacturable and integrative method and equipment with short processing time and high reproducibility for large-scale preparing flexible sensors of mechanical bending durability on flexible substrates. This preparation method is scalable and silver electrodes can be replaced with other metallic materials such as gold, copper, chromium, indium tin oxide (ITO), aluminum oxide, and so forth. We believe that this method provides a new route to short-time and quantifiably fabricate IPMC sensors for potential wearable applications in real-time monitoring human motion and human−machine interaction.

EXPERIMENTAL METHODS

Materials and Instruments. Hydrogen peroxide, sulfuric acid, $HAuCl_4$, 1,10-phenanthroline monohydrate (Phen), and sodium sulfite were purchased from Sinopharm Chemical Regent Co. Ltd. The Nafion 117 membrane was purchased from the Dupont. Equipment with the commercial dc balanced magnetron sputtering system and the inductive coupled plasma-reactive ion etcher was customized.

DOI: 10.1021/acsomega.8b00877
ACS Omega 2018, 3, 9146−9154

Preparation of the IPMC Sensor by in Situ Plasma Etching and Magnetron Sputtering Depositing. Before etching, the Nafion membrane was cleaned by hydrogen peroxide (5% mass fraction) and diluted sulfuric acid (1 mol L^{-1}). Then, the Nafion membrane (suitable for different size) was fixed on the hollow part of the rotatable sample holder in the chamber allowing the rotation at a speed of 5 rpm of the substrate along a direction, which assures sample uniformity of etching and metallizing over the entire surface. The chamber pressure was pumped down to below 3×10^{-4} pa in order to prevent residual atmosphere effects on the composition of the Nafion films. Then, the argon valve was opened and the argon flow rate was set as 8 sccm. All of the specimens were grown by using pure argon (99.99%) as etching and sputtering gas. We controlled the screen voltage, the screen current, and etching duration during plasma etching to get a sample with uniform etching and excellent performance. After completing treatment of one side of the Nafion membrane, the holder was turned over 180° by the mechanical handle, and the opposite side of the membrane was etched. Then, magnetron sputtering deposited silver particles on the metallic polymer. The sputtering process was performed at room temperature. The chamber pressure was adjusted to appropriate value. The argon flow rate was set to what we want. Then, the deposition power and duration parameters were set. Once the deposition was completed, the holder was turned over 180° by the mechanical handle, and the opposite side of the polymer was processed. No post annealing was performed after deposition. The substrate temperature was maintained at 20 °C approximately during the deposition process. The Nafion membrane is cleaned with ionized water, vacuumed in the chamber, etched, and sputtered to plate the electrodes. The Nafion membrane retains its intrinsic water, which assures the migration of ions in the membrane, thereby generating the sensing signal. The IPMC sensor was cut into a size of 25 mm × 5 mm for the experimental test.

Preparation of the Electroless Plating-Based Sensor. The Nafion membrane was roughed by 1200 sandpaper polishing 800 times both sides. Then, the Nafion membrane was cleaned. Next step, the Nafion membrane was placed into a solution of $[Au(Phen)Cl_2]Cl$ for 24 h to allow the sufficient impregnation of cations. After that, the Nafion membrane was immersed into deionized water in water-bath heating. A Na_2SO_3 solution of 5 mmol L^{-1} was slowly dropped into the water till the Au cations at the membrane's surface are reduced to Au particles totally. The impregnation−reduction steps were repeated five times.

Sensing Measurement. The IPMC sensors need to be deformed to produce a voltage signal. We built a corresponding test platform, including signal generation section and signal collection section. The signal generation section includes fixtures, displacement platform (MTS121), and displacement stepper motor. The signal collection section includes an electrochemical workstation and a controller computer. The displacement platform can realize precise displacement control in the *X*-axis direction, with an accuracy of 0.005 mm. Moreover, the displacement platform can realize and control different movement rates, the number of cycle displacements, and the distance of displacement, including any distance of 0−7 mm. The electrochemical workstation can collect and display on the computer the electrical signals generated by the deformation of the sensor. Therefore, we can use this measurement platform to realize the basic bending performance test of our sensor. The IPMC sensor in response to the cyclic bending and resuming flat state is tested. The sensor is placed on the displacement platform and is clamped by fixtures. The sensors we test have an effective length of 1.8 cm. Also, the maximum displacement of the platform is set as 3 mm. The displacement platform gradually moves from 0 to 3 mm, the signal generated by the sensor gradually increases from 0, and then the displacement platform gradually returns from 3 to 0 mm. The signal generated by the sensor gradually decreases from the maximum value.

Characterization. Surface morphology and cross-sectional SEM images were obtained with a Hitachi S-4800 filed emission scanning electron microscope. The 3D AFM images and the average rms surface roughness (R_q) values were obtained with a Dimension 3100 atomic force microscope. EDX was performed on Quanta 400FEG (FEI). XRD patterns were obtained on a X'Pert-Pro MPD (Cu Kα). The surface sheet resistance of the electrode film was tested by using a multifunctional digital four-probe tester (ST-2258C).

■ ASSOCIATED CONTENT

Supporting Information

The Supporting Information is available free of charge on the ACS Publications website at DOI: 10.1021/acsomega.8b00877.

Picture of a simple holder; schematic diagram of analytical model of the sensor; potential change of IPMC under overtime state maintaining; and electromechanical behavior of IPMC under electrical voltage stimulation of ±3 V (PDF)

■ AUTHOR INFORMATION

Corresponding Author

*E-mail: wchen2006@sinano.ac.cn (W.C.).

ORCID

Wei Chen: 0000-0001-9527-110X

Notes

The authors declare no competing financial interest.

■ ACKNOWLEDGMENTS

This work was supported by the External Cooperation Program of BIC from Chinese Academy of Sciences (grant no. 121E32KYSB20130009) and the Science and Technology of Jiangsu Province (grant no. BE2016086).

■ REFERENCES

(1) Ge, J.; Sun, L.; Zhang, F.-R.; Zhang, Y.; Shi, L.-A.; Zhao, H.-Y.; Zhu, H.-W.; Jiang, H.-L.; Yu, S.-H. A Stretchable Electronic Fabric Artificial Skin with Pressure-, Lateral Strain-, and Flexion-Sensitive Properties. *Adv. Mater.* **2016**, *28*, 722−728.

(2) Liao, C.; Zhang, M.; Yao, M. Y.; Hua, T.; Li, L.; Yan, F. Flexible Organic Electronics in Biology: Materials and Devices. *Adv. Mater.* **2015**, *27*, 7493−7527.

(3) Park, M.; Park, Y. J.; Chen, X.; Park, Y.-K.; Kim, M.-S.; Ahn, J.-H. MoS2 -Based Tactile Sensor for Electronic Skin Applications. *Adv. Mater.* **2016**, *28*, 2556−2562.

(4) Zang, Y.; Huang, D.; Di, C.-a.; Zhu, D. Device Engineered Organic Transistors for Flexible Sensing Applications. *Adv. Mater.* **2016**, *28*, 4549−4555.

(5) Chortos, A.; Liu, J.; Bao, Z. Pursuing prosthetic electronic skin. *Nat. Mater.* **2016**, *15*, 937−950.

DOI: 10.1021/acsomega.8b00877
ACS Omega 2018, 3, 9146−9154

(6) Chen, K.; Gao, W.; Emaminejad, S.; Kiriya, D.; Ota, H.; Nyein, H. Y. Y.; Takei, K.; Javey, A. Printed Carbon Nanotube Electronics and Sensor Systems. *Adv. Mater.* **2016**, *28*, 4397−4414.
(7) Hwang, S.-W.; Lee, C. H.; Cheng, H.; Jeong, J.-W.; Kang, S.-K.; Kim, J.-H.; Shin, J.; Yang, J.; Liu, Z.; Ameer, G. A.; Huang, Y.; Rogers, J. A. Biodegradable elastomers and silicon nanomembranes/nanoribbons for stretchable, transient electronics, and biosensors. *Nano Lett.* **2015**, *15*, 2801−2808.
(8) Takei, K.; Takahashi, T.; Ho, J. C.; Ko, H.; Gillies, A. G.; Leu, P. W.; Fearing, R. S.; Javey, A. Nanowire active-matrix circuitry for low-voltage macroscale artificial skin. *Nat. Mater.* **2010**, *9*, 821−826.
(9) Hammock, M. L.; Chortos, A.; Tee, B. C.-K.; Tok, J. B.-H.; Bao, Z. 25th anniversary article: The evolution of electronic skin (e-skin): a brief history, design considerations, and recent progress. *Adv. Mater.* **2013**, *25*, 5997−6038.
(10) Lee, S. G.; Park, H. C.; Pandita, S. D.; Yoo, Y. Performance Improvement of IPMC (Ionic Polymer Metal Composites) for a Flapping Actuator. *Int. J. Contr. Autom. Syst.* **2006**, *4*, 748−755.
(11) Shahinpoor, M.; Bar-Cohen, Y.; Xue, T.; Harrison, J. S.; Smith, J. Ionic Polymer-Metal Composites (IPMCs) as Biomimetic Sensors, Actuators and Artificial Muscles: A Review. *ACS Symposium* **1999**, *7* (6), 251−267.
(12) Lee, S.; Kim, K. J.; Park, H. C. Modeling of an IPMC Actuator-driven Zero-Net-Mass-Flux Pump for Flow Control. *J. Intell. Mater. Syst. Struct.* **2006**, *17*, 533−541.
(13) Shahinpoor, M.; Kim, K. J. Ionic polymer−metal composites: IV. Industrial and medical applications. *Smart Mater. Struct.* **2005**, *14*, 197−214.
(14) Shahinpoor, M.; Kim, K. J. Ionic polymer−metal composites: III. Modeling and simulation as biomimetic sensors, actuators, transducers, and artificial muscles. *Smart Mater. Struct.* **2004**, *13*, 1362−1388.
(15) Park, K.; Lee, H.-K. Evaluation of circuit models for an IPMC (Ionic Polymer-Metal Composite) sensor using a parameter estimate method. *J. Korean Phys. Soc.* **2012**, *60*, 821−829.
(16) Pugal, D.; Jung, K.; Aabloo, A.; Kim, K. J. Ionic polymer−metal composite mechanoelectrical transduction: review and perspectives. *Polym. Int.* **2010**, *59*, 279−289.
(17) Kim, K. J.; Shahinpoor, M. Ionic polymer metal composites: II. Manufacturing techniques. *Smart Mater. Struct.* **2003**, *12*, 65−79.
(18) Zhu, H.; Wang, X.; Liang, J.; Lv, H.; Tong, H.; Ma, L.; Hu, Y.; Zhu, G.; Zhang, T.; Tie, Z.; Liu, Z.; Li, Q.; Chen, L.; Liu, J.; Jin, Z. Versatile Electronic Skins for Motion Detection of Joints Enabled by Aligned Few-Walled Carbon Nanotubes in Flexible Polymer Composites. *Adv. Funct. Mater.* **2017**, *27*, 1606604.
(19) Liu, Q.; Chen, J.; Li, Y.; Shi, G. High-Performance Strain Sensors with Fish-Scale-Like Graphene-Sensing Layers for Full-Range Detection of Human Motions. *ACS Nano* **2016**, *10*, 7901−7906.
(20) Park, H.; Jeong, Y. R.; Yun, J.; Hong, S. Y.; Jin, S.; Lee, S.-J.; Zi, G.; Ha, J. S. Stretchable Array of Highly Sensitive Pressure Sensors Consisting of Polyaniline Nanofibers and Au-Coated Polydimethylsiloxane Micropillars. *ACS Nano* **2015**, *9*, 9974−9985.
(21) Liu, Y.; Hu, Y.; Zhao, J.; Wu, G.; Tao, X.; Chen, W. Self-Powered Piezoionic Strain Sensor toward the Monitoring of Human Activities. *Small* **2016**, *12*, 5074−5080.
(22) Balakrisnan, B.; Nacev, A.; Smela, E. Design of bending multilayer electroactive polymer actuators. *Smart Mater. Struct.* **2015**, *24*, 045032.
(23) Shahinpoor, M.; Kim, K. J. The effect of surface-electrode resistance on the performance of ionic polymer-metal composite (IPMC) artificial muscles. *Smart Mater. Struct.* **2000**, *9*, 543−551.
(24) Yan, Y.; Santaniello, T.; Bettini, L. G.; Minnai, C.; Bellacicca, A.; Porotti, R.; Denti, I.; Faraone, G.; Merlini, M.; Lenardi, C.; Milani, P. Electroactive Ionic Soft Actuators with Monolithically Integrated Gold Nanocomposite Electrodes. *Adv. Mater.* **2017**, *29*, 1606109.
(25) Omosebi, A.; Besser, R. S. Electron beam assisted patterning and dry etching of Nafion membranes. *J. Electrochem. Soc.* **2011**, *158*, D603−D610.
(26) Van Nguyen, T.; Vu Nguyen, M.; Nordheden, K.; He, W. Effect of bulk and surface treatments on the surface ionic activity of nafion membranes. *J. Electrochem. Soc.* **2007**, *154*, A1073−A1076.
(27) Bar-Cohen, Y.; Zhou, W.; Li, W. J.; Xi, N.; Ma, S. *Development of Force-Feedback-Controlled Nafion Micromanipulators*, 2001; Vol. *4329*, p 401.
(28) Siripong, M.; Fredholm, S.; Nguyen, Q. A. A cost-effective fabrication method for ionic polymer-metal composites. *MRS Online Proc. Libr.* **2005**, *889*, 0889−W04-03.
(29) Grace, J. M.; Gerenser, L. J. Plasma Treatment of Polymers. *J. Dispersion Sci. Technol.* **2003**, *24*, 305−341.
(30) Kitova, S.; Minchev, M.; Malinowski, J. Soft plasma treatment of polymer surfaces. *J. Optoelectron. Adv. Mater.* **2005**, *7*, 249−252.
(31) Helmersson, U.; Lattemann, M.; Bohlmark, J.; Ehiasarian, A. P.; Gudmundsson, J. T. Ionized physical vapor deposition (IPVD): A review of technology and applications. *Thin Solid Films* **2006**, *513*, 1−24.
(32) Song, D. S.; Han, D. G.; Rhee, K.; Kim, D. M.; Jho, J. Y. Fabrication and characterization of an ionic polymer-metal composite bending sensor. *Macromol. Res.* **2017**, *25*, 1205−1211.
(33) Hwang, D.-K.; Bang, K.-H.; Jeong, M.-C.; Myoung, J.-M. Effects of RF power variation on properties of ZnO thin films and electrical properties of p−n homojunction. *J. Cryst. Growth* **2003**, *254*, 449−455.
(34) Cho, Y.-H.; Bae, J. W.; Cho, Y.-H.; Lim, J. W.; Ahn, M.; Yoon, W.-S.; Kwon, N.-H.; Jho, J. Y.; Sung, Y.-E. Performance enhancement of membrane electrode assemblies with plasma etched polymer electrolyte membrane in PEM fuel cell. *Int. J. Hydrogen Energy* **2010**, *35*, 10452−10456.
(35) Song, D.; Aberle, A. G.; Xia, J. Optimisation of ZnO:Al films by change of sputter gas pressure for solar cell application. *Appl. Surf. Sci.* **2002**, *195*, 291−296.

DOI: 10.1021/acsomega.8b00877
ACS Omega 2018, 3, 9146−9154